

# Grain Boundary Faceting and Abnormal Grain Growth in Nickel

SUNG BO LEE, NONG MOON HWANG, DUK YONG YOON, and MICHAEL F. HENRY

A correlation between grain boundary faceting and abnormal grain growth has been observed in recrystallized polycrystalline Ni at varying annealing temperatures, with or without C added. Carburized Ni specimens deformed to 50 pct show faceted grain boundaries and abnormal grain growth when annealed at temperatures below  $0.7 T_m$ , where  $T_m$  is the melting point of Ni in absolute scale. When annealed at or above  $0.7 T_m$ , the grain boundaries are smoothly curved and, therefore, have a rough structure, and normal grain growth is observed. In the specimens annealed in vacuum without carburization, all grain boundaries are faceted at  $0.55 T_m$ , and some of them become defaceted at higher temperatures. The specimens annealed in vacuum at temperatures between  $0.55$  and  $0.95 T_m$  show abnormal grain growth. When the grain boundaries have a rough structure and are, therefore, nearly isotropic, normal grain growth is indeed expected, as shown by the simulation and analytical treatment. When all or a fraction of the grain boundaries are faceted, with the facet planes corresponding to the singular cusp directions in the variation of the boundary energy against the inclination angle, abnormal grain growth can occur either because some grain boundary junctions become immobile due to a torque effect, or the growth occurs by a step mechanism.

## I. INTRODUCTION

THE abnormal grain growth (AGG) or secondary recrystallization in alloys has been attributed to textures<sup>[1,2]</sup> or grain boundary pinning by precipitates<sup>[3,4,5]</sup> and, in thin films, to anisotropic surface energy.<sup>[6,7,8]</sup> But AGG has also been observed in highly pure bulk polycrystals of Ag,<sup>[9,10]</sup> Cd,<sup>[11]</sup> Cu,<sup>[10,12,13]</sup> Ni,<sup>[14]</sup> Fe,<sup>[15]</sup> Pb,<sup>[11]</sup> Pd,<sup>[10]</sup> and Sn.<sup>[16]</sup> It was also observed in the specimens where no texture was found or expected to exist.<sup>[10,13]</sup> The AGG in pure or single-phase bulk polycrystals has been attributed to segregation of impurity or additive solute atoms at grain boundaries.<sup>[17,18,19]</sup>

The purpose of this work is to explore the possible relation of the grain boundary structure and its transformation to AGG in a bulk polycrystal of pure metal without any texture. During the last few decades, the possibility of a grain boundary roughening transformation has been proposed<sup>[20,21]</sup> and verified experimentally by mostly indirect methods.<sup>[22–27]</sup> But, except possibly for the rare cases of the grain boundaries with orientations (inclination angles) corresponding to cusps in the polar plot of the grain boundary energy ( $\gamma$ ) vs inclination angle, the grain boundaries are expected to undergo facet-defacet transformation, as pointed out by Cahn.<sup>[28]</sup> Indeed, both general grain boundaries in polycrystalline materials and grain boundaries with well-defined geometrical characteristics such as the coincidence site lattice (CSL) relations were observed to have faceted structures<sup>[29–34]</sup> and

to undergo reversible defaceting transformation.<sup>[35]</sup> Impurities and additives were also found to induce grain boundary faceting.<sup>[36–42]</sup>

If grain boundaries are faceted, the facet planes or a fraction of them can be singular, with ordered structures corresponding to cusp directions in the  $\gamma$  plot vs the inclination angle. The grains with faceted boundaries may, thus, have a different growth behavior from those with defaceted rough boundaries. Various possible mechanisms for linking the AGG behavior to the grain boundary structure are examined in this work. Grain boundaries are likely to have a rough structure at temperatures close to the melting point, and oxygen has been reported to induce grain boundary faceting in Ni,<sup>[42]</sup> which is used in this work. There are indications from previous observations that AGG is indeed related to grain boundary faceting. Simpson *et al.*<sup>[11]</sup> observed apparently normal grain growth in pure Cd, Pb, and their dilute alloys at temperatures close to their melting points after isochronal anneals, but suggested that AGG had occurred at early stages. Gleiter<sup>[43]</sup> observed structural transformations of grain boundaries, which probably were faceting transformations, as pointed out by Cahn,<sup>[28]</sup> in zone-refined Pb and noted that, below the transformation temperatures, AGG occurred. Recently, Randle and Horton<sup>[14]</sup> reported that normal grain growth occurred in Ni at temperatures close to the melting point, and, at relatively low temperatures, more pronounced AGG was observed in an impure Ni than in a pure Ni specimen. Because they presented the grain structures after annealing for several hours, it is not clear if AGG had not occurred at early stages for the apparently normal growth structures. They suggested that grain boundary structural transformation was the cause for the apparent dependence of the growth behavior on the specimen purity and the annealing temperature, but did not specify or observe the boundary transformation.

In this work, the grain growth behavior of recrystallized Ni is observed at various temperatures for various annealing periods under a low vacuum and a carburizing atmosphere.

SUNG BO LEE, Postdoctoral Research Associate, and DUK YONG YOON, Professor, are with the Department of Materials Science and Engineering, Korea Advanced Institute of Science and Technology, Taejeon 305-701, Korea. NONG MOON HWANG, Sub Group Leader, is with the National Creative Research Initiative Center for Microstructure Science of Materials, College of Engineering, Seoul National University, Seoul 151-742, Korea; also Principal Investigator, Korea Research Institute of Standard and Science, Taejeon 305-600, Korea. MICHAEL F. HENRY, Metallurgist, is with the General Electric Research and Development Center, Niskayuna, NY 12309.

Manuscript submitted June 18, 1999.

The grain boundary shapes are examined under transmission electron microscopy to establish a correlation to the growth behavior.

## II. EXPERIMENTAL PROCEDURE

Commercial grade (Ni 270) Ni rods of 1.2 cm in diameter and 99.97 wt pct purity were used in this experiment. The concentrations of C and S were determined by an elemental analyzer and those of the metallic impurities by an inductively coupled plasma atomic emission spectrometer. Some Ni pieces were carburized by heating in sealed quartz tubes containing packs of BaCO<sub>3</sub> and graphite, in equal weight, at 1100 °C for 100 hours. The Ni rods were compressed to a 50 pct reduction of length to about 1 cm. They were annealed in either a vacuum of 10<sup>-4</sup> to 10<sup>-5</sup> Torr or in the same atmosphere as that used for the carburizing at temperatures between 0.55  $T_m$  (677 °C) and 0.95  $T_m$  (1365 °C), where  $T_m$  is the melting point of Ni in absolute scale. The specimens were rapidly pushed into the center of a tube-type annealing furnace which was set at a desired temperature. After the annealing treatment, the specimens were rapidly pulled out of the furnace. The annealed rods were sectioned through the center perpendicular to the axes for microscopic observations. The polished specimens were etched in a solution of 50 ml hydrochloric acid, 50 ml ethyl alcohol, 50 ml water, and 10 g cupric sulfate. The grain boundary morphology was examined by a transmission electron microscope (TEM). The grain size was measured by tracing along grain boundaries on micrographs using a digitizer connected to a personal computer. The sizes of about 150 to 200 grains were measured in each specimen. The surface structure of the grains in the specimens, which were polished with fine (0.05  $\mu$ m) alumina powder before annealing, was also examined under a scanning electron microscope (SEM).

## III. RESULTS AND DISCUSSION

Both AGG and grain boundary faceting were observed to depend on the presence of carbon and the annealing temperature. Most of the results of this work are summarized in Figure 1. In the carburized specimens, normal grain growth occurred at temperatures above 0.7  $T_m$  (936 °C) and AGG occurred below 0.7  $T_m$ . In the specimens annealed under vacuum, AGG occurred at all temperatures between 0.55 and 0.95  $T_m$ . Except during the early incubation period, all or a fraction of the grain boundaries in the specimens showing AGG were faceted. In contrast, all of the grain boundaries in the specimens showing normal grain growth were defaceted, with smoothly curved or nearly straight grain boundaries. Thus, a correlation was found between the grain boundary faceting and AGG.

Some heat-treatments, particularly at relatively high temperatures, were carried for periods as short as 30 seconds. The solution of the temperature rise of the specimen using the standard radiative heat-transfer equation<sup>[44]</sup> showed that, at 0.7 and 0.95  $T_m$ , the specimen temperatures were expected to reach the set furnace temperatures in about 0.3 and 0.1 seconds, respectively. We will first describe the observations in the carburized specimens. The carbon content in the as-received Ni was determined to be about 20 ppm, and that

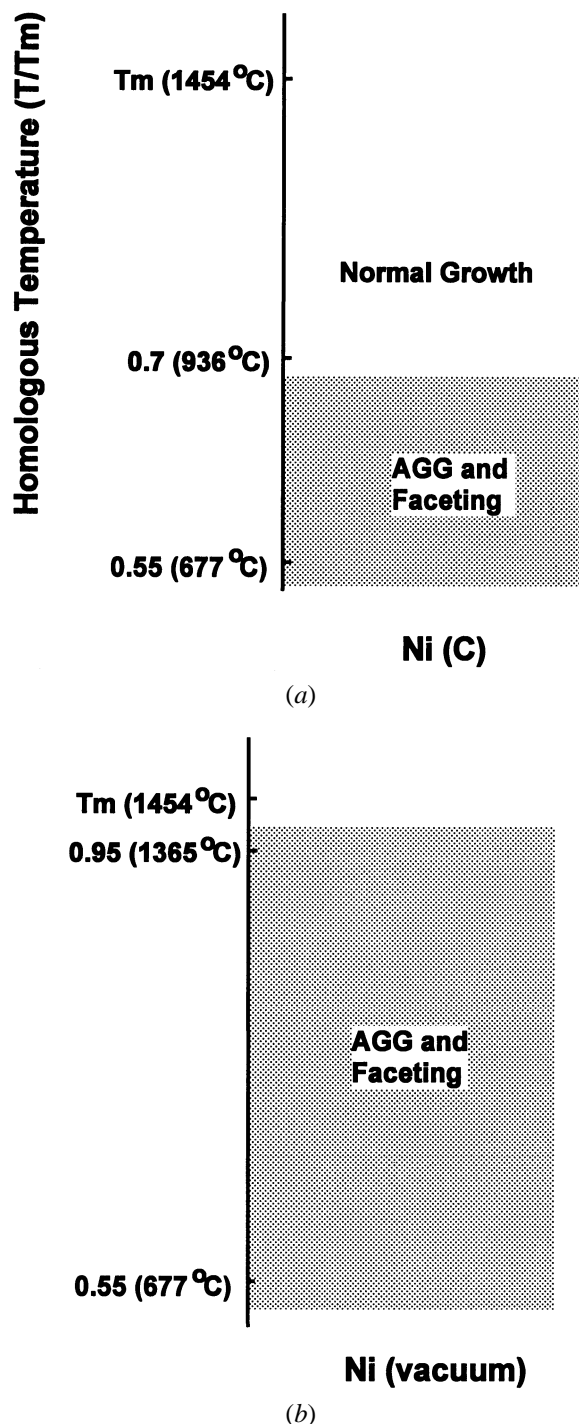


Fig. 1—The observed dependence of AGG and grain boundary faceting on annealing temperature in (a) carburizing atmosphere and (b) vacuum.

in carburized specimens about 800 ppm, by weight. The X-ray pole figures of the recrystallized specimens did not show any texture, as expected of metals deformed to 50 pct. Each specimen examined in this study will be designated by the temperature/period/atmosphere of its annealing treatment. Thus, for example, a specimen annealed at 0.55  $T_m$  for 10 minutes in a carburizing atmosphere will be designated as 0.55  $T_m$ /10 min/C. This specimen showed recrystallized grains which had apparently undergone some coarsening,

but there were no distinct, abnormally large grains, as exhibited in Figure 2(a). The specimen annealed for 50 minutes at this temperature had some grains beginning to grow to large sizes, as shown in Figure 2(b). Thus, there appeared to be an incubation period of about 50 minutes for AGG under this annealing condition. The specimen annealed for 90 minutes, shown in Figure 2(c), had very large grains exceeding  $1000\ \mu\text{m}$  and fine matrix grains of approximately the same size as the grains shown in Figure 2(a). The carburized specimens annealed at  $0.6\ T_m$  ( $763\ ^\circ\text{C}$ ) also showed AGG, but the incubation period appeared to be shorter than that for those annealed at  $0.55\ T_m$ . The  $0.6\ T_m/35\ \text{min/C}$  specimen has an AGG structure similar to the  $0.55\ T_m/90\ \text{min/C}$  specimen, shown in Figure 2(c).

In the specimen annealed at  $0.55\ T_m$  for 10 minutes (before the onset of AGG, as shown in Figure 2(a)), all of the 17 grain boundaries examined showed defaceted and slightly curved shapes. But, in the  $0.55\ T_m/50\ \text{min/C}$  specimen shown in Figure 2(b), six out of the 13 grain boundaries examined were faceted, as shown in Figure 3. It was, thus, possible

to observe some faceted grain boundaries meeting smoothly curved grain boundaries at triple junctions, as shown in Figure 3(b). Because the incoherent twin boundaries have step structures which resemble the faceted boundaries, the orientations of the two grains across the faceted boundaries were checked by electron diffraction under a TEM. In all the specimens with AGG structures, the TEM observations of the grain boundary shapes were made on the relatively fine matrix grains, because it was nearly impossible to hit upon the boundary of a large grain. But, after long annealing treatments, some of the grain boundaries between the large abnormally grown grains, which impinged upon each other and probably grew slightly further, had facet structures sufficiently coarse to be seen under an optical microscope, as shown in Figure 4 for the  $0.6\ T_m/2\ \text{h/C}$  specimen.

These observations at  $0.55\ T_m$  indicate that, after the primary recrystallization, the grain boundaries have defaceted shapes and develop faceting during the incubation period of about 50 minutes for AGG. Even after prolonged annealing treatments, only a fraction of the boundaries can be faceted,

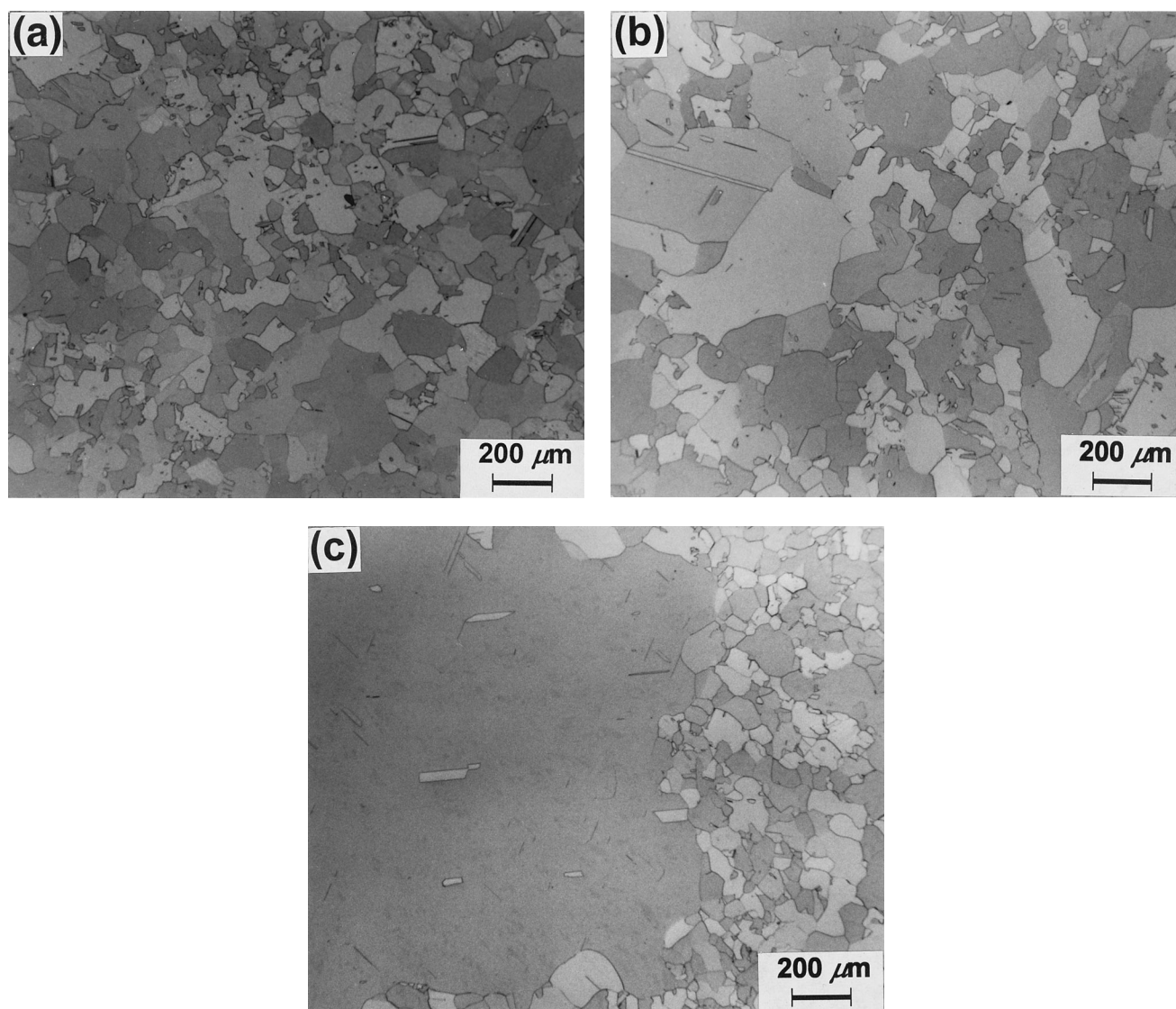


Fig. 2—The optical microstructures of the carburized specimens annealed at  $0.55\ T_m$  for (a) 10 min, (b) 50 min, and (c) 90 min.

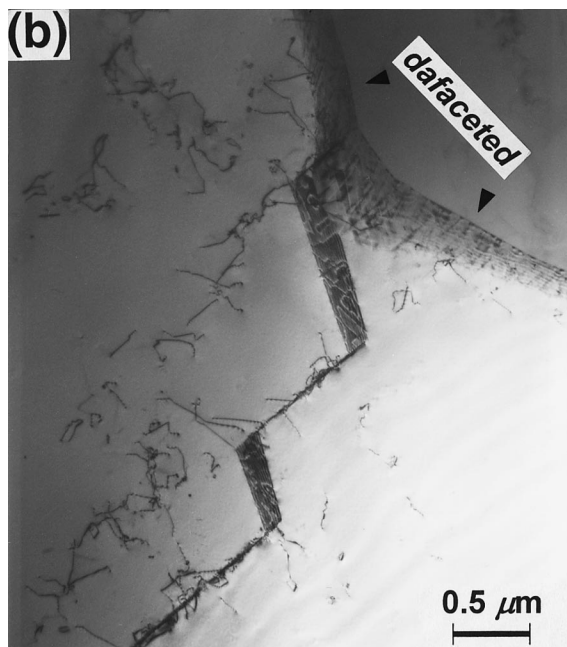
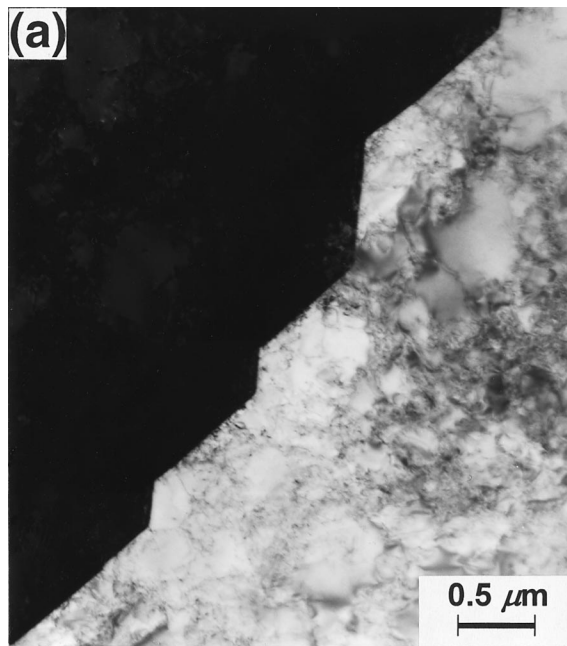


Fig. 3—The TEM micrographs of (a) a faceted grain boundary and (b) a faceted grain boundary meeting two defaceted grain boundaries at a triple junction in the  $0.55 T_m/50 \text{ min/C}$  specimen.

apparently because the transformation temperatures vary among the grain boundaries.

As noted earlier and shown in Figure 1, the grains in the carburized specimens appeared to undergo normal growth at  $0.7 T_m$  and above. The evolutions of the microstructure and the grain size distribution at  $0.8 T_m$  ( $1109^\circ\text{C}$ ) are shown in Figures 5 and 6, respectively. During 30 seconds at this temperature (Figure 5(a)), the primary recrystallization appears to have been completed, and, after 1 minute (Figure 5(b)), the steady-state grain shape had not yet been developed. After annealing further for 3 and 10 minutes, normal growth structures were observed, as shown in Figures 5(c)

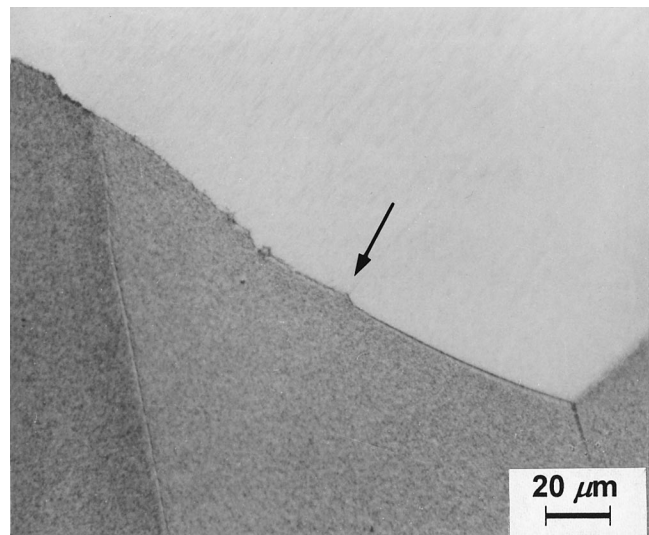


Fig. 4—The optical micrograph of a faceted grain boundary (indicated by an arrow) in the  $0.6 T_m/2 \text{ h/C}$  specimen.

and (d), respectively. Although the measured grain size distributions in Figure 6 are not smooth because of the limited number of grains, they resemble those typically observed in normal grain growth. The grain growth patterns at  $0.7$  and  $0.9 T_m$  were similar to that at  $0.8 T_m$ , shown in Figure 5, but the growth rate increased with temperature. The carburized specimens were annealed for longer periods of up to 2 hours at  $0.7$ ,  $0.8$ , and  $0.9 T_m$ , and there was no microstructure which could be identified as AGG at any stage of the annealing treatment.

The grain boundaries in these specimens were examined under a TEM at relatively early stages of the annealing treatment, when the grains were small. The optical microstructure of the  $0.7 T_m/2 \text{ min/C}$  specimen resembled Figure 5(b), and all of the nine grain boundaries examined were smoothly curved, as shown in Figure 7. The optical microstructure of the  $0.9 T_m/2 \text{ min/C}$  specimens resembled Figure 5(c), and all of the seven grain boundaries examined under the TEM were also smoothly curved. The grains in the specimens annealed for 1 or 2 hours were so large that the TEM observation was difficult, but their optical micrographs showed smoothly curved boundaries, as can be seen in Figure 5(d). The stepped boundaries were all incoherent twin boundaries, and there was no grain boundary with a coarse faceted structure, like that shown in Figure 4, for the specimen annealed at  $0.6 T_m$  for 2 hours.

The surfaces of the carburized specimens were also examined under an SEM after the annealing treatments at  $0.6 T_m$  and above, and they were found to be smooth without any faceted hill-and-valley structure. At  $0.6 T_m$ , some grain boundaries were faceted, as shown in Figure 4, and the defaceting transition temperatures for the grain boundary and surface are expected to be different.

Because the grains after the completion of the primary recrystallization have somewhat irregular shapes and size distributions, as shown in Figures 5(a) and (b), there is some ambiguity in determining their growth behavior at the early stages of growth. In order to overcome this difficulty and to verify the temperature dependence of the growth behavior,

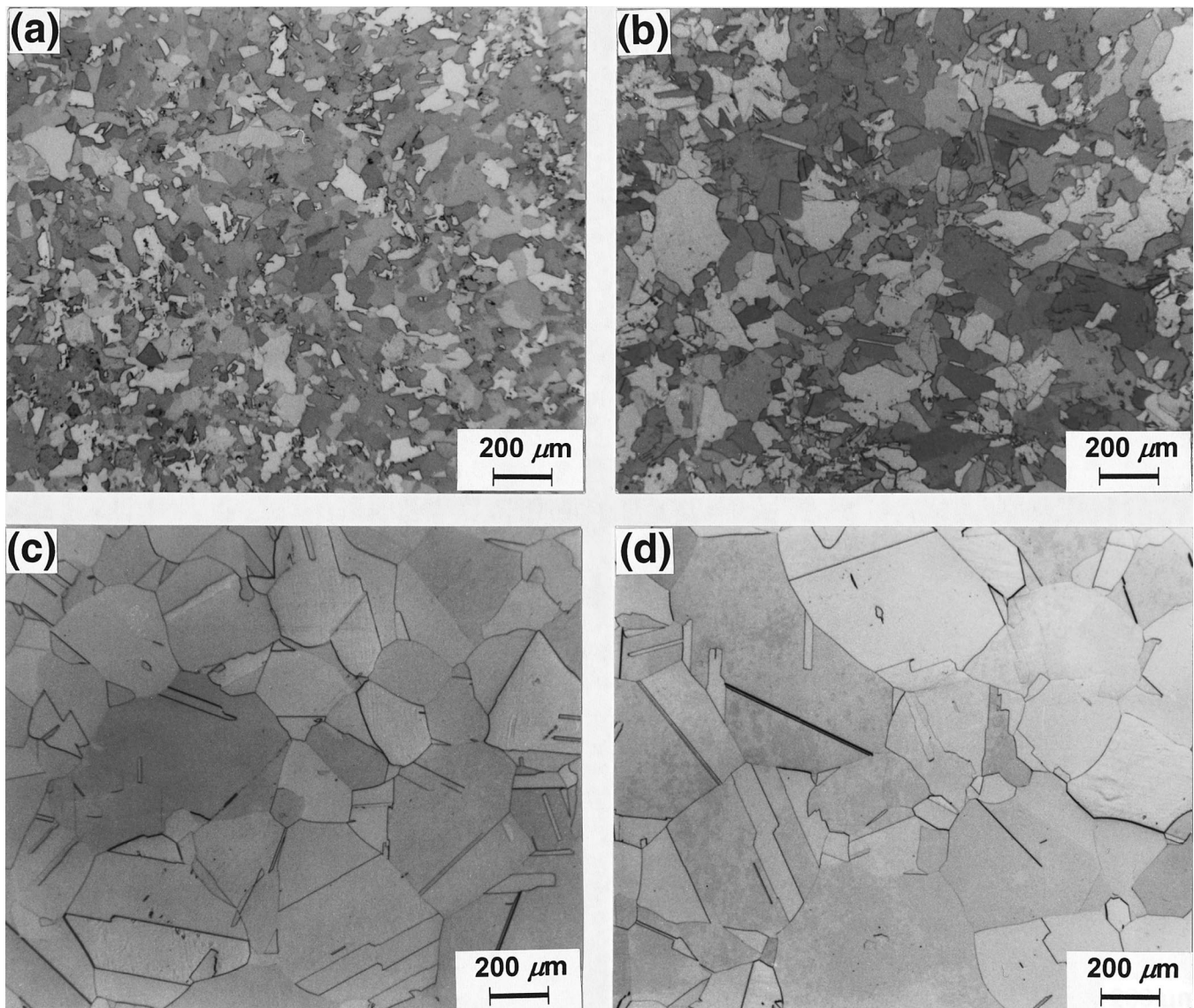


Fig. 5—The optical microstructures of the carburized specimens annealed at  $0.8 T_m$  for (a) 30 s, (b) 1 min, (c) 3 min, and (d) 10 min.

the specimens were annealed in steps at two temperatures where normal and abnormal growth behaviors were expected, according to Figure 1. In the first experiment, a carburized specimen was annealed at  $0.55 T_m$  for 50 minutes to obtain the AGG structure shown in Figure 2(b) and was again annealed at  $0.9 T_m$  for 3 minutes. During the annealing treatment at  $0.9 T_m$ , the fine matrix grains grew, and a normal growth structure resembling that obtained by annealing at  $0.9 T_m$  for 3 minutes (without the first annealing treatment at  $0.55 T_m$ ) was observed, as shown in Figure 8(a). If this double annealed specimen was annealed for longer periods at  $0.9 T_m$ , the grains would have continued to grow normally. In the second experiment, a carburized specimen was first annealed at  $0.9 T_m$  for 30 seconds to obtain a recrystallized structure resembling that in Figure 5(a). When the specimen was annealed again at  $0.55 T_m$  for 30 minutes, a typical AGG structure was obtained, as shown in Figure 8(b). The results of these double annealing experiments thus confirm that the grain growth mode, either normal or abnormal, for

the carburized specimens depends on the annealing temperature, as illustrated in Figure 1.

All the specimens annealed in vacuum in the temperature range between  $0.55$  and  $0.95 T_m$  used in this work showed AGG, as summarized in Figure 1. But, the incubation time for AGG was shorter than that for the carburized specimens. The specimen annealed in vacuum at  $0.55 T_m$  for 10 minutes, for example, showed a distinct AGG structure. In contrast, the carburized specimens showed an AGG structure after annealing for 50 minutes at  $0.55 T_m$ , as shown in Figure 2(b), and the grain size distribution obtained after annealing for 30 minutes in vacuum at  $0.55 T_m$  was similar to that obtained after 90 minutes at the same temperature, in the carburized specimen shown in Figure 2(c). Randle and Horton<sup>[14]</sup> observed that Ni specimens of 99.5 wt pct purity showed a slightly abnormal grain size distribution after annealing in vacuum for 6 hours at  $0.64 T_m$  and normal size distributions at  $0.68$ ,  $0.72$ , and  $0.76 T_m$ . The specimens of 99.999 wt pct purity showed a distinct AGG structure after



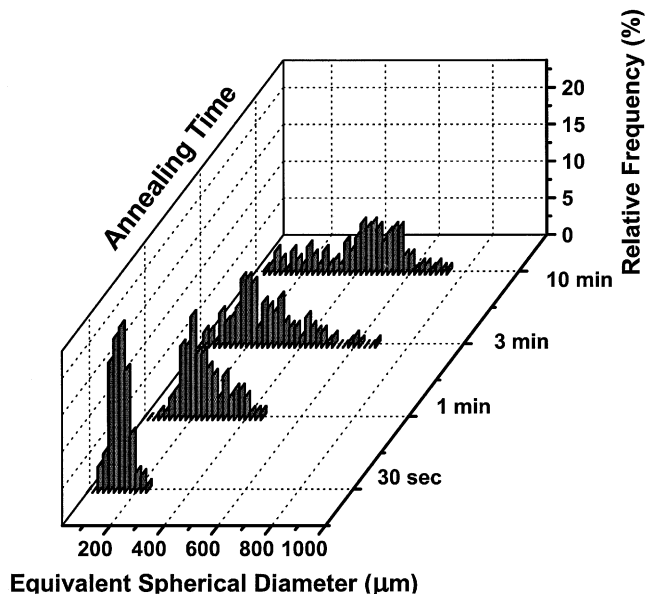


Fig. 6—The measured grain size distributions of the specimens shown in Fig. 5.

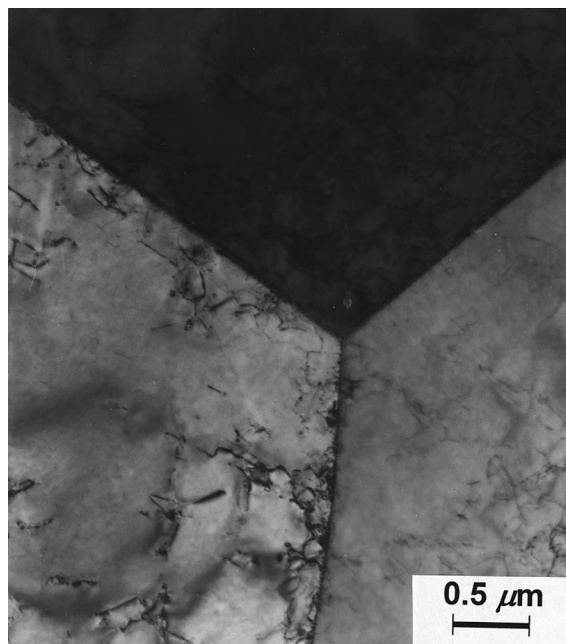


Fig. 7—The TEM micrograph of three defaceted grain boundaries meeting at a triple junction in the  $0.7 T_m/2 \text{ min/C}$  specimen.

annealing for 4 hours at  $0.68 T_m$  and a normal size distribution at  $0.76 T_m$ . Because they reported observations after relatively long annealing treatments, the growth behavior of their specimens at the earlier stages is not clear, but the difference from the results of this work may arise from the differences in the impurities and the initial grain size.

The incubation time for AGG appeared to decrease with increasing annealing temperature. The specimen annealed in vacuum at  $0.95 T_m$  for 1 minute, for example, showed a distinct AGG structure, as exhibited in Figure 9. With increasing annealing temperature there were more abnormally growing grains, and they impinged against each other

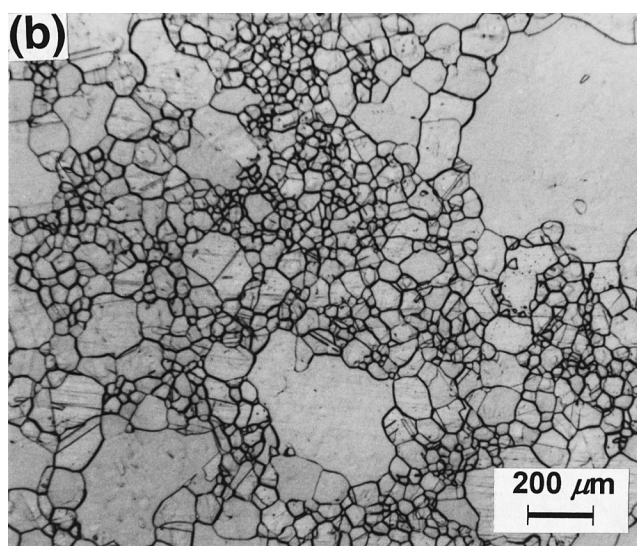
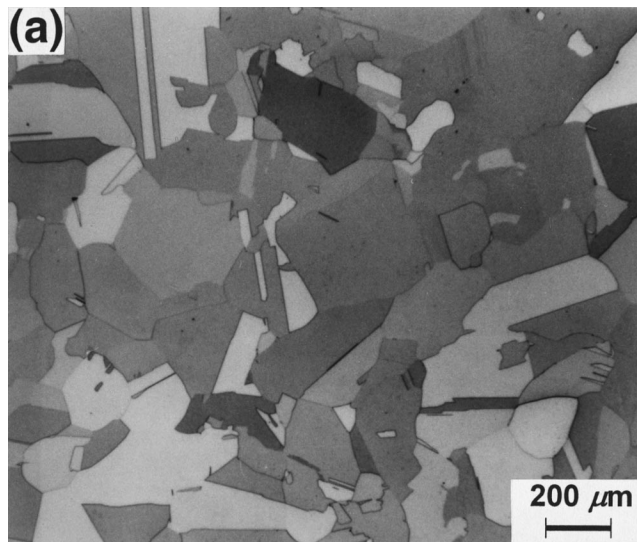


Fig. 8—The optical microstructures of the carburized specimens (a) annealed at  $0.55 T_m$  for 50 min and again at  $0.9 T_m$  for 3 min, and (b) annealed at  $0.9 T_m$  for 30 s and again at  $0.55 T_m$  for 30 min.

sooner. Thus, the abnormally growing grains after their impingement were smaller at higher annealing temperatures.

All or a fraction of the grain boundaries examined in each specimen annealed in vacuum were faceted, and the fraction of the faceted boundaries appeared to decrease with increasing temperature. For examples, all of the seven grain boundaries examined under a TEM in the  $0.6 T_m/7 \text{ min/v}$  specimen were faceted, but only four out of the ten grain boundaries examined in the  $0.95 T_m/1 \text{ min/v}$  specimen were faceted, and the rest were smoothly curved. Most of the facet planes appeared to be flat, but there were some which appeared to be slightly curved. Most of the junctions between the facet planes appeared to be sharp, but some appeared to be rounded, although obviously the exact shape of these junctions could not be accurately resolved at these magnifications. After long annealing treatments, the large impinged AGG grains showed some coarse faceted structures which could be observed even under optical microscope, as exhibited in Figure 10. A similar coarse faceted structure was

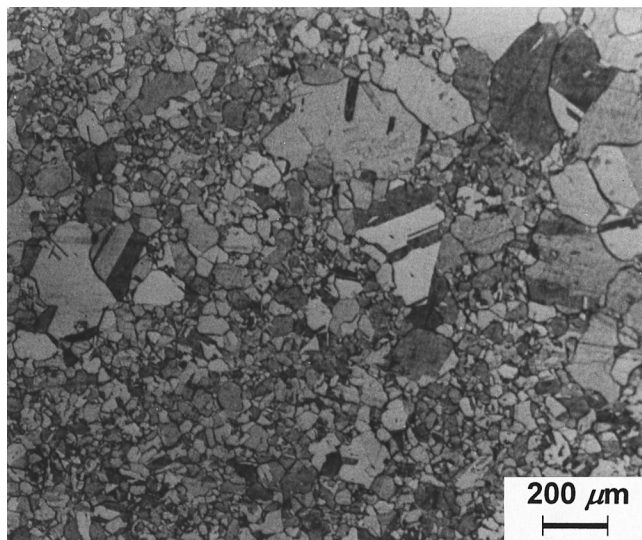


Fig. 9—The optical microstructure of the specimen annealed in vacuum at  $0.95 T_m$  for 1 min.

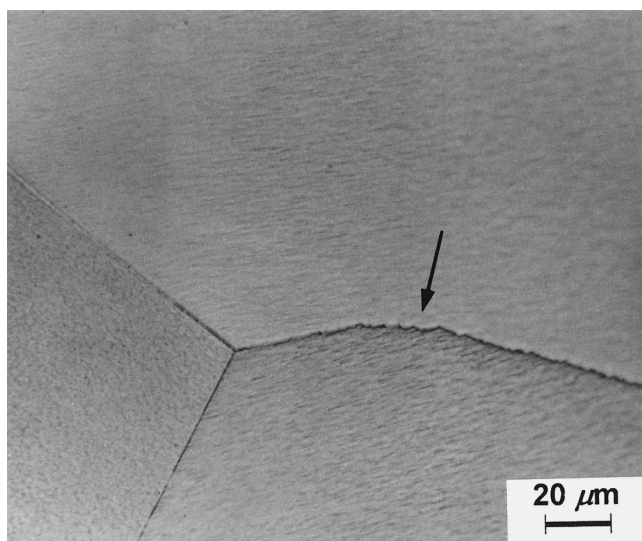


Fig. 10—The optical micrograph of a faceted grain boundary (indicated by an arrow) at a triple junction in the  $0.8 T_m/2$  h/v specimen.

shown in Figure 4 for the carburized specimen annealed at  $0.6 T_m$  for 2 hours.

The surface structure of grains was also examined under an SEM in the specimens which were annealed for long periods. The  $0.6 T_m/96$  h/v and  $0.8 T_m/48$  h/v specimens showed single grains with faceted hill-and-valley structures at the surfaces, but the  $0.9 T_m/12$  h/v specimen showed striated step structures at the surface of some grains, while, at others, the surface appeared to be smooth. These results, thus, show that the surface faceting of the grains also depends on the annealing temperature and the presence of carbon.

The grain boundary faceting in Ni, which appears to be closely related to the occurrence of AGG, was previously observed by Henry *et al.*,<sup>[42]</sup> and their results are largely consistent with the present observations. In a commercial grade Ni, they observed faceted grain boundaries when slowly cooled, but smoothly curved grain boundaries when

quenched after heat-treatment at  $1050\text{ }^{\circ}\text{C}$  ( $0.77 T_m$ ). The intergranular fracture surface in a specimen heat-treated at  $650\text{ }^{\circ}\text{C}$  ( $0.53 T_m$ ) showed distinct grain boundary facet planes. By examining the effect of atmosphere changes from hydrogen to argon, they concluded that the faceting was induced by oxygen. The faceted grain boundaries were also observed in recrystallized Nb<sup>[45]</sup> and in Al and Cu<sup>[46]</sup> sheets. The addition of Te or Bi to Fe<sup>[36,37]</sup> or Cu,<sup>[38–41]</sup> respectively, was observed to induce grain boundary faceting. On the other hand, the addition of MgO to Al<sub>2</sub>O<sub>3</sub> was observed to induce defaceting.<sup>[47]</sup> Gjostein<sup>[48]</sup> and Shewmon and Robertson<sup>[49]</sup> proposed that the impurities or additives segregating at steps or terraces (singular planes) of a crystal surface would induce defaceting or faceting, respectively, but presently there is no theory which can predict the effect of impurities or additives on the faceting of a surface or a grain boundary. The defaceting effect of carbon addition observed in this work may arise from its reaction with oxygen or directly from its segregation at grain boundaries.

More systematic studies of grain boundary faceting were previously performed on grain boundaries with well defined misorientations, often of the CSL relations, between the grains. Hsieh and Balluffi<sup>[35]</sup> observed in a hot-stage electron microscope that CSL grain boundaries in Al and Au thin films underwent reversible faceting-defaceting transformations in the range between  $0.54$  and  $0.96 T_m$ . The present study shows that the general grain boundaries in a polycrystalline material with random misorientations (between the grains and random average boundary orientation (inclination angle)) also undergo faceting transformation with temperature change as well as with additives.

The thermodynamic principles of the faceting of grain boundaries and crystal surfaces are identical. The faceting of a grain boundary is described by the variation of the grain boundary energy ( $\gamma$ ) with the direction of the grain boundary normal, represented as the inclination angle. Herring<sup>[50]</sup> showed that the faceting into a hill-and-valley structure occurs if the average surface or grain boundary orientation does not correspond to an orientation which appears in the equilibrium shape, or, as Frank<sup>[51]</sup> showed, if it falls into the concave region of the reciprocal  $\gamma$  plot. As pointed out by Cahn,<sup>[28]</sup> the facet-defacet transformation is of the first-order type, which is analogous to the decomposition reaction in ternary alloys. Experimentally, the faceting has been mainly observed for the grain boundaries between grains of CSL misorientations and with tilt angles around low index axes. Although some facets were found to correspond to the low energy boundaries predicted by the CSL model,<sup>[32,34]</sup> others did not agree with the CSL model or with any other model based on geometrical relationships.<sup>[31,33,34,52]</sup>

Presently, there is no theory which describes the  $\gamma$  plot and its dependence on temperature for a grain boundary of an arbitrary misorientation angle. The observations of Henry *et al.*<sup>[42]</sup> and of the present study that all grain boundaries in polycrystalline Ni at low temperatures, in the presence of oxygen, are faceted indicate that the  $\gamma$  plots for any misorientation angle are strongly anisotropic, likely with deep cusps. Some facet planes are, thus, likely to correspond to the singular boundaries of the cusp orientations. If the reciprocal  $\gamma$  plot has smoothly varying convex regions corresponding to curved regions in the equilibrium shape, some of the randomly selected grain boundaries with these surface

normals will be defaceted. In analogy to the decomposition reaction in ternary systems,<sup>[28]</sup> the curved facet planes sometimes observed in this work may arise from the orientation gradient which can exist before the equilibrium flat facet planes are developed. The rounded edges between the facet planes can arise from spinodal faceting.<sup>[28]</sup>

If the faceted boundary planes are singular with ordered structures, their thermodynamic and kinetic characteristics might be quite different from those of the rough boundaries and may determine the grain growth behavior. One can consider several possible mechanisms for the causal relation between grain boundary faceting and AGG. The first is the grain growth stagnation when singular grain boundaries meet at triple junctions. Recently, King<sup>[53]</sup> proposed that singular grain boundaries corresponding to cusp orientations in the  $\gamma$  plot can meet other grain boundaries, either singular or rough, with ranges of dihedral angles, because ranges of values of the grain boundary torque or, equivalently, the capillarity vector are possible, as pointed out earlier by Herring<sup>[50]</sup> and Hoffman and Cahn.<sup>[54]</sup> When such equilibria are established at triple junctions, grain growth can be inhibited because the grain boundary curvatures can disappear. It is then possible that, at the junctions which are not in equilibrium, the grains can grow abnormally.

The next possible mechanism for linking the grain boundary faceting to AGG is related to the migration kinetics of the faceted grain boundaries. Various theories for the atomic process of the grain boundary movement have been proposed, but do not take into account the possibility of grain boundary structural change, which became known only recently. If one or all of the facet planes of a grain boundary are singular with an orientation corresponding to a cusp in the  $\gamma$  plot, it may move by the step mechanism, similar to the growth of a faceted crystal in a melt.<sup>[55]</sup> Gleiter<sup>[55]</sup> showed that, with this mechanism, the grain boundary velocity will vary linearly or parabolically with the driving energy when it is low, but, when it is very high, the velocity will increase exponentially with the driving energy. Such a sharp increase of the velocity with the driving energy can cause AGG, as proposed by Park *et al.*<sup>[56]</sup> for the faceted grains dispersed in a liquid matrix growing by two-dimensional nucleation. For crystal growth, it has been proposed that, for large driving forces greater than that required for two-dimensional nucleation at the surface, the atom attachment to the growing surface will be rapid and, hence, the velocity will again increase linearly with the driving force.<sup>[57,58]</sup> Cahn<sup>[59]</sup> proposed a general theory of such a possibility for any type of boundary. Temkin's multilayer model<sup>[60]</sup> for a solid-liquid interface predicted a similar growth behavior of crystals from the melt. Although such a nonlinear increase of the grain boundary velocity with the driving energy and sudden increases of the velocity at particular temperatures have been observed by Sun and Bauer<sup>[61]</sup> and others,<sup>[19,62]</sup> the results were explained by the impurity segregation effect. But, it is possible that some of these behaviors stem from grain boundary faceting.

Another possible reason for the correlation between AGG and grain boundary faceting is that impurity segregation causes both AGG and grain boundary faceting and, hence, there is no direct causal relationship between AGG and the faceting. Impurities segregating at grain boundaries can

retard the migration, but if the driving force is large, the grain boundaries can break away from the impurity atoms and, thus, move with a relatively large intrinsic mobility, as proposed by Cahn<sup>[63]</sup> and Lucke and Stuwe.<sup>[64]</sup> The velocity is, thus, predicted to increase sharply at a certain driving force, similar to that predicted for the step mechanism. Such behaviors have, indeed, been observed, as noted earlier, in NaCl<sup>[61]</sup> and Fe-3 wt pct Si bicrystals,<sup>[62]</sup> and AGG of Fe-3 wt pct Si polycrystals has been attributed to the segregation effect of S, N, and B<sup>[17,18]</sup> at grain boundaries. The AGG in oxide dispersion-strengthened Ni-base superalloys<sup>[19]</sup> has also been attributed to the segregation of solute atoms.

As noted earlier, Henry *et al.*<sup>[42]</sup> showed that grain boundary faceting in Ni was induced by oxygen, and the defaceting effect of carbon observed in the present work can be attributed either to the reaction with oxygen or segregation at grain boundaries. On the other hand, the Ni used in the present work was found to contain about 0.01 wt pct each of Co and Cr (and smaller amounts of Fe, Cu, and Mg). Because Co and Cr are expected to diffuse more slowly than O or C in Ni, they may retard the normal grain growth and determine the AGG behavior, according to the prediction of Cahn.<sup>[63]</sup> Therefore, if AGG in Ni arose from the impurity segregation at grain boundaries, it will be largely independent of the O and C concentrations, in contradiction to the observations. It has to be, thus, concluded that the correlation between AGG and the boundary faceting observed in Ni is not an accidental one which stems from the impurity segregation at grain boundaries.

Finally, the correlation between AGG and the boundary faceting may be attributed to the grain boundary anisotropy, which is implied by the faceting. If grain boundaries are defaceted with smoothly curved shapes, as shown in Figure 7 for those in Ni at high temperatures in a carburizing atmosphere, they will have disordered structures and, hence, be nearly isotropic in their boundary energy and other properties. The Monte Carlo simulation of Srolovitz *et al.*<sup>[65]</sup> showed that a two-dimensional polycrystal with isotropic grain boundary energy exhibited normal grain growth behavior, even when a large grain was embedded in the matrix of fine grains. This conclusion was confirmed by an analytical treatment of Thompson *et al.*<sup>[66]</sup> for a polycrystalline system with isotropic grain boundary energy and a grain size distribution predicted by Lifshitz and Slyozov<sup>[67]</sup> and Wagner<sup>[68]</sup> for interface-controlled growth. Rios<sup>[69]</sup> later pointed out that AGG behavior was possible if the matrix grain size distribution was narrow. The present observations show that the grains grow normally if the boundaries are nearly isotropic, in agreement with the simulation and analysis of Srolovitz *et al.*<sup>[65]</sup> and Thompson *et al.*<sup>[66]</sup>

Grest *et al.*<sup>[70]</sup> also performed the Monte Carlo simulation of two-dimensional grains, with the grain boundary energy varying with the misorientation angle between grains of randomly distributed orientations, and their results show a small change of the growth behavior without any indication of AGG with increasing degree of boundary energy anisotropy. Only in the systems with textures did the computer simulations predict AGG if the grain boundaries were anisotropic.<sup>[71,72]</sup> It, thus, appears that without any texture, the anisotropy of the grain boundary energy itself does not cause AGG.



## IV. CONCLUSIONS

These observations show that, if all grain boundaries have a rough structure and, therefore, a nearly isotropic normal grain, growth occurs. When all or a fraction of the grain boundaries are faceted, abnormal grain growth is observed to occur. There appear to be two possible mechanisms for linking the faceted grain boundary to AGG. The first is the junction stability with singular boundaries, proposed by King,<sup>[53]</sup> and the second is the step growth<sup>[55]</sup> which becomes continuous at high driving forces.<sup>[59]</sup> More work is needed to establish the causal relationship between the grain boundary faceting and AGG. The atomic structure of the faceted grain boundaries with general misorientation relations needs to be examined, both theoretically and experimentally, to elucidate the nature of the singularity at certain inclination angles. The migration kinetics of the faceted and the rough grain boundaries should be also examined in, for example, bicrystals. A general boundary can be either rough or singular, and the grain boundary properties can strongly depend on these two possible grain boundary states. The normal or the abnormal growth appears to be one of them. The correlation between AGG and the grain boundary faceting has also been observed in a number of other polycrystalline materials and will be reported later.

## ACKNOWLEDGMENTS

This work was supported by the Corporate Research and Development Center, General Electric Company, and by the Korea Ministry of Science and Technology through the Nanostructure Technology Project. Two of the authors (SBL and NMH) were supported by the Creative Research Initiative Center for Microstructure Science of Materials during the final phase of this work.

## REFERENCES

1. C.G. Dunn: *Acta Metall.*, 1953, vol. 1, pp. 163-75; *Acta Metall.*, 1954, vol. 2, pp. 173-83.
2. C.G. Dunn and J.L. Walter: in *Recrystallization, Grain Growth and Textures*, H. Margolin, ed., ASM, Metals Park, OH, 1966, pp. 461-521.
3. M. Hillert: *Acta Metall.*, 1965, vol. 13, pp. 227-38.
4. J. Calvet and C. Renon: *Mem. Sci. Rev. Metall.*, 1960, vol. 57, pp. 345-62.
5. T. Gladman: *Proc. R. Soc. London A*, 1966, vol. A294, pp. 298-309.
6. J.L. Walter: *Acta Metall.*, 1959, vol. 7, pp. 424-26.
7. M. McLean and H. Mykura: *Acta Metall.*, 1965, vol. 13, pp. 1291-97.
8. H.J. Frost, C.V. Thompson, and D.T. Walton: *Acta Metall. Mater.*, 1992, vol. 40, pp. 779-93.
9. F.D. Rosi, B.H. Alexander, and C.A. Dube: *Trans. TMS-AIME*, 1952, vol. 152, pp. 189-96.
10. B. Gunther, A. Kumpmann, and H.-D. Kunze: *Scripta Metall. Mater.*, 1992, vol. 27, pp. 833-38.
11. C.J. Simpson, K.T. Aust, and W.C. Winegard: *Metall. Trans.*, 1971, vol. 2, pp. 987-91.
12. M.L. Kronberg and F.H. Wilson: *Trans. TMS-AIME*, 1949, vol. 185, pp. 501-14.
13. V.Y. Gertsman and R. Birringer: *Scripta Metall. Mater.*, 1994, vol. 30, pp. 577-81.
14. V. Randle and D. Horton: *Scripta Metall. Mater.*, 1994, vol. 31, pp. 891-95.
15. G. Riontino, C. Antonione, L. Battezzati, F. Marino, and M. Tabasso: *J. Mater. Sci.*, 1979, vol. 14, pp. 86-90.
16. E.L. Holmes and W.C. Winegard: *Acta Metall.*, 1959, vol. 7, pp. 411-14.
17. H.E. Grenoble: *IEEE Trans. Mag.*, 1977, Mag. 13, pp. 1427-32.
18. H.C. Fiedler: *Metall. Trans. A*, 1977, vol. 8A, pp. 1307-12.
19. C.P. Jongenberger and R.F. Singer: in *New Materials by Mechanical Alloying Techniques*, E. Arzt and L. Shultz, eds., DGM, Erlangen, 1989, pp. 157-74.
20. E.W. Hart: *The Nature and Behavior of Grain Boundaries*, H. Hu, ed., Plenum Press, New York, NY, 1972, pp. 155-70; M. Guttmann: *Metall. Trans. A*, 1977, vol. 8A, pp. 1383-1401.
21. C. Rottman: *Phys. Rev. Lett.*, 1986, vol. 57, pp. 735-38.
22. H. Sautter, H. Gleiter, and G. Baro: *Acta Metall.*, 1977, vol. 25, pp. 467-73.
23. U. Erb and H. Gleiter: *Scripta Metall.*, 1979, vol. 13, pp. 61-64.
24. E.M. Fridman, C.V. Kopecky, and L.S. Shvindlerman: *Z. Metallkd.*, 1975, vol. 66, pp. 533-39.
25. L.S. Shvindlerman and B.B. Straumal: *Acta Metall.*, 1985, vol. 33, pp. 1735-49.
26. E.L. Maksimova, L.S. Shvindlerman, and B.B. Straumal: *Acta Metall.*, 1988, vol. 36, pp. 1573-83.
27. E.L. Maksimova, E.I. Rabkin, L.S. Shvindlerman, and B.B. Straumal: *Acta Metall.*, 1989, vol. 37, pp. 1995-98.
28. J.W. Cahn: *J. Phys. Colloq.*, 1982, No. 12, pp. 199-213.
29. E.L. Hall, J.L. Walter, and C.L. Briant: *Phil. Mag. A*, 1982, vol. 45A, pp. 753-70.
30. M.D. Vaudin, M. Ruhle, and S.L. Sass: *Acta Metall.*, 1983, vol. 31, pp. 1109-16.
31. P. Viswanathan and C.L. Bauer: *Metall. Trans.*, 1973, vol. 4, pp. 2645-50.
32. W.R. Wagner, T.Y. Tan, and R.W. Balluffi: *Phil. Mag.*, 1974, vol. 29, pp. 895-904.
33. M.S. Masteller and C.L. Bauer: *Phil. Mag. A*, 1978, vol. 38A, pp. 697-706.
34. P.J. Goodhew, T.Y. Tan, and R.W. Balluffi: *Acta Metall.*, 1978, vol. 26, pp. 557-67.
35. T.E. Hsieh and R.W. Balluffi: *Acta Metall.*, 1989, vol. 37, pp. 2133-39.
36. J.R. Rellick, C.J. McMahon, H.L. Marcus, and P.W. Palmberg: *Metall. Trans.*, 1971, vol. 2, p. 1492-94.
37. C. Pichard, J. Rieu, and C. Goux: *Mem. Sci. Rev. Metall.*, 1973, vol. 70, pp. 13-22.
38. A.M. Donald and L.M. Brown: *Acta Metall.*, 1979, vol. 27, pp. 59-66.
39. A. Donald: *Phil. Mag.*, 1976, vol. 34, pp. 1185-89.
40. T.G. Ference and R.W. Balluffi: *Scripta Metall.*, 1988, vol. 22, pp. 1929-34.
41. M. Menyhard, B. Blum, and C.J. McMahon, Jr.: *Acta Metall.*, 1989, vol. 37, pp. 549-57.
42. G. Henry, J. Plateau, X. Wache, M. Gerber, I. Behar, and C. Crussard: *Mem. Sci. Rev. Metall.*, 1959, vol. 56, pp. 417-26.
43. H. Gleiter: *Z. Metallkd.*, 1970, vol. 61, pp. 282-87.
44. D.R. Poirier and G.H. Geiger: *Transport Phenomena in Materials Processing*, TMS, Warrendale, PA, 1994, pp. 369-415.
45. A.V. Andrejeva, G.I. Salnikov, and L.K. Fionova: *Acta Metall.*, 1978, vol. 26, pp. 1331-36.
46. A.V. Andrejeva and L.K. Fionova: *Fiz. Met. Metall.*, 1981, vol. 52, pp. 593-603.
47. C.W. Park: Korea Advanced Institute of Science and Technology, Taejeon, private communication, 1998.
48. G.A. Gjostein: *Acta Metall.*, 1963, vol. 11, pp. 957-67.
49. P.G. Shewmon and W.M. Robertson: in *Metal Surfaces*, W.D. Robertson and N.A. Gjostein, eds., ASM, Metals Park, OH, 1963, pp. 67-98.
50. C. Herring: *Phys. Rev.*, 1951, vol. 82, pp. 87-93; in *Structure and Properties of Solid Surfaces*, R. Gomer and C.S. Smith, eds., University of Chicago Press, Chicago, 1953, pp. 5-81.
51. F.C. Frank: in *Metal Surfaces*, W.D. Robertson and N.A. Gjostein, eds., ASM, Metals Park, OH, 1963, pp. 1-15.
52. A.P. Sutton and R.W. Balluffi: *Acta Metall.*, 1987, vol. 35, pp. 2177-2201.
53. A.H. King: *Grain Growth in Polycrystalline Materials III*, Proc. 3rd Int. Conf. on Grain Growth, H. Weiland, B.L. Adams and A.D. Rollett, eds., TMS, Warrendale, PA, 1998, pp. 333-38.
54. D.W. Hoffman and J.W. Cahn: *Surf. Sci.*, 1972, vol. 31, pp. 368-88; J.W. Cahn and D.W. Hoffman: *Acta Metall.*, 1974, vol. 22, pp. 1205-14.
55. H. Gleiter: *Acta Metall.*, 1969, vol. 17, pp. 565-73.
56. Y.J. Park, N.M. Hwang, and D.Y. Yoon: *Metall. Mater. Trans. A*, 1996, vol. 27A, pp. 2809-19.
57. D.P. Woodruff: *The Solid-Liquid Interface*, Cambridge University Press, London, 1973, pp. 151-73.

58. K.A. Jackson and B. Chalmers: *Can. J. Phys.*, 1956, vol. 34, pp. 473-90.
59. J.W. Cahn: *Acta Metall.*, 1960, vol. 8, pp. 554-62.
60. D.E. Temkin: in *Crystallization Processes*, N.N. Sirota, F.K. Gorskii, and V.M. Varikash, eds., English translation published by Consultants Bureau, New York, NY, 1966.
61. R.C. Sun and C.L. Bauer: *Acta Metall.*, 1970, vol. 18, pp. 639-47.
62. S. Tsurekawa, T. Ueda, K. Ichikawa, H. Nakashima, Y. Yoshitomi, and H. Yoshinaga: *Mater. Sci. Forum*, 1996, vols. 204-206, pp. 221-26.
63. J.W. Cahn: *Acta Metall.*, 1962, vol. 10, pp. 789-98.
64. K. Lucke and H.P. Stuwe: *Recovery and Recrystallization of Metals*, L. Himmel, ed., Interscience, New York, NY, 1963, pp. 171-210.
65. D.J. Srolovitz, G.S. Grest, and M.P. Anderson: *Acta Metall.*, 1985, vol. 33, pp. 2233-47.
66. C.V. Thompson, H.J. Frost, and F. Spaepen: *Acta Metall.*, 1987, vol. 35, pp. 887-90.
67. I.M. Lifshitz and V.V. Slyozov: *J. Phys. Chem. Solids*, 1961, vol. 19, pp. 35-50.
68. C. Wagner: *Z. Electrochem.*, 1961, vol. 65, pp. 581-91.
69. P.R. Rios: *Acta Metall. Mater.*, 1992, vol. 40, pp. 2765-68.
70. G.S. Grest, D.J. Srolovitz, and M.P. Anderson: *Acta Metall.*, 1985, vol. 33, pp. 509-20.
71. A.D. Rollett, D.J. Srolovitz, and M.P. Anderson: *Acta Metall.*, 1989, vol. 37, pp. 1227-40.
72. N.M. Hwang: *J. Mater. Sci.*, 1998, vol. 33, pp. 5625-29.